Metaheuristics-based LPV Controller Synthesis with Uncertainty Volume Maximization

Rémi Pédenon-Orlanducci[1] and Philippe Feyel[2] and David Saussié[1]

***Abstract*— Uncertain Linear-Parameter-Varying (LPV) systems in both polytopic and Linear-Fractional-Representation (LFT) frameworks are studied. Gain-scheduled robust controllers designed for such systems typically exhibit degraded $\mathscr{H}_\infty$ performance when uncertainty variation ranges are large. Conversely, small uncertainty ranges allow for good performance but result in overly conservative adaptive controllers that are impractical in real applications. To address this trade-off, a method is proposed that simultaneously maximizes the admissible uncertainty variation range and the achievable performance level, formulated as an optimization problem. The problem is solved using a metaheuristic algorithm, and the effectiveness of the approach is demonstrated on two benchmark case studies.**

I. Introduction

In adaptive robust control, the synthesis of an LPV gain-scheduled (GS) controller relies on the knowledge of the bounds of uncertain parameters, both in the LFT and polytopic frameworks [1]. This raises the fundamental question of whether priority should be given to performance or to tolerance with respect to uncertainty. In other words, it becomes necessary to strike a balance between ensuring high performance, measured in terms of $\mathscr{L}_2$-gain, and maintaining model generality, expressed in terms of the admissible range of uncertain parameters. This perspective also provides a means of monitoring situations where varying uncertainties exceed their admissible domain, as encountered in identification [2].

The objective of this work is to develop a method that simultaneously maximizes the uncertainty volume and controller performance in LPV–LFT and polytopic LPV systems. To this end, a nonconvex optimization problem is formulated, where the decision variables are the scalings that ensure the existence of a robust GS controller [3, 4] and the uncertainty bounds in the LFT framework, and the uncertainty bounds alone in the polytopic framework. This problem is formulated through a single objective optimization problem and solved using a metaheuristic algorithm, specifically Particle Swarm Optimization (PSO) [5], allowing the robust GS controller to be computed offline while avoiding the limitations of LMI-based methods [6].

Previous works have addressed uncertainty volume maximization, but only in the context of robustness post-analysis, such as μ-analysis [7], *i.e.*, with unknown yet static parameters. Although this approach is promising in the LFT framework, no polytopic formulation has been proposed and no controller has been synthesized. Other theoretical approaches studying the maximal uncertain set exist (through stability radius for instance, see [8]) but – to the best of the author's knowledge – none of them use the LPV framework. In the present paper, the uncertainty bounds remain unknown, but the uncertainties are time-varying. The main challenge is therefore to determine the optimal controller state-space while simultaneously maximizing the uncertainty volume that can be stabilized by the designed controller.

The paper is organized as follows. Section II introduces the robust controller synthesis problem together with the standard notations, and presents the overall framework of the contribution. Section III formulates the optimization problem and discusses numerical solution methods. Section IV reports two benchmark studies: a mechatronic system with high stability margins and six uncertain parameters, used to illustrate the LFT approach; and a cart-pendulum system from the literature, characterized by smaller stability margins and two varying parameters, used to illustrate the polytopic approach. Results are presented for each benchmark, together with a discussion of computational aspects.

II. Problem statement

A. Preliminaries

First, some notations and useful definitions are introduced. The definitions in this section are adapted from [9].

Definition 1 ($\mathbb{L}_2$-norm and $\mathbb{L}_2$-space): Let $f:\mathbb{R}_+\to\mathbb{C}^n$ be a function. The $\mathbb{L}_2$ norm is defined as

$$\|f\|_2 := \sqrt{\int_0^\infty f(t)^* f(t)\mathrm{d}t}, \tag{1}$$

and the $\mathbb{L}_2$ space is defined as the set of finite-energy signals:

$$\mathbb{L}_2 := \{f:\mathbb{R}_+\to\mathbb{C}^n,\ \|f\|_2<\infty\}. \tag{2}$$

We denote by $\mathbb{L}_2^*$ the set of non-zero functions of $\mathbb{L}_2$.

Definition 2 ($\mathscr{L}_2$-gain): Let G be a bounded operator from $\mathbb{L}_2$ to $\mathbb{L}_2$, *i.e.*, $\forall f\in\mathbb{L}_2, \|Gf\|_2<\infty$ holds. Its $\mathscr{L}_2$-gain, denoted $\|G\|_{\mathscr{L}_2}$, is defined by

$$\|G\|_{\mathscr{L}_2} := \sup_{f\in\mathbb{L}_2^*}\frac{\|Gf\|_2}{\|f\|_2}. \tag{3}$$

Definition 3 ($\mathscr{H}_\infty$-norm): Let $\widehat{G}:\mathbb{C}\to\mathbb{C}^{m\times q}$ be a proper transfer function, analytic in the closed right-half plane. The $\mathscr{H}_\infty$-norm of this transfer function, denoted by $\|\widehat{G}\|_\infty$, is defined by:

$$\|\widehat{G}\|_\infty := \sup_{\omega\in\mathbb{R}}\overline{\sigma}(\widehat{G}(j\omega)), \tag{4}$$

[1]Rémi Pédenon-Orlanducci and David Saussié are with Mobile Robotics and Autonomous Systems Laboratory, Faculty of Electrical Engineering, Polytechnique Montréal, QC H3T 0A3 Montréal, Canada {remi.pedenon-orlanducci,d.saussie}@polymtl.ca

[2]Philippe Feyel is with Safran Trusted 4D Canada, QC H3A 3M8 Montréal, Canada philippe.feyel@safrangroup.com

where $\overline{\sigma}(\cdot)$ denotes the maximal singular-value.

With these notations, the $\mathscr{L}_2$-gain of an LTI operator is the same as the $\mathscr{H}_\infty$-norm of its transfer function, *i.e.*, $\|G\|_{\mathscr{L}_2} = \|\widehat{G}\|_\infty$. Hence, the LTI system G is asymptotically stable if and only if it has finite $\mathscr{L}_2$-gain, which is also equivalent to its transfer function $\widehat{G}$ having finite $\mathscr{H}_\infty$-norm.

B. LPV framework

Both LPV-LFT and polytopic LPV frameworks shall be presented. The LFT form is more general and less conservative, yet more difficult to formulate mathematically; whereas the polytopic one is often quite easily obtained mathematically but can lead to more conservative results as coupled parameters will remain within a subvolume of the polytope, besides it is more heavy numerically as the controller synthesis implies LMI resolution at each vertex of the polytope.

1) LPV-LFT framework: Consider a plant P in the LPV-LFT framework, as given by (5).

$$\begin{bmatrix} \dot{\mathbf{x}}(t) \\ \mathbf{z}_\Delta(t) \\ \mathbf{z}(t) \\ \mathbf{y}(t) \end{bmatrix} = \begin{bmatrix} \mathbf{A} & \mathbf{B}_\Delta & \mathbf{B}_1 & \mathbf{B}_2 \\ \mathbf{C}_\Delta & \mathbf{D}_{\Delta\Delta} & \mathbf{D}_{\Delta 1} & \mathbf{D}_{\Delta 2} \\ \mathbf{C}_1 & \mathbf{D}_{1\Delta} & \mathbf{D}_{11} & \mathbf{D}_{12} \\ \mathbf{C}_2 & \mathbf{D}_{2\Delta} & \mathbf{D}_{21} & \mathbf{0} \end{bmatrix} \begin{bmatrix} \mathbf{x}(t) \\ \mathbf{w}_\Delta(t) \\ \mathbf{w}(t) \\ \mathbf{u}(t) \end{bmatrix}, \tag{5a}$$

$$\mathbf{w}_\Delta(t) = \Delta(t)\mathbf{z}_\Delta(t), \tag{5b}$$

with $\mathbf{x} \in \mathbb{R}^n$ the state vector; $\mathbf{w}_\Delta, \mathbf{z}_\Delta \in \mathbb{R}^{n_\Delta}$ the perturbation input and output vectors, respectively; $\mathbf{w} \in \mathbb{R}^{n_w}$ the exogenous input; $\mathbf{z} \in \mathbb{R}^{n_z}$ the performance output; $\mathbf{u} \in \mathbb{R}^{n_u}$ the control input; and $\mathbf{y} \in \mathbb{R}^{n_y}$ the measured output. The matrix $\Delta(t) \in \mathbb{R}^{n_\Delta \times n_\Delta}$ denotes the uncertainty matrix.

A common approach is to assume that all plant matrices depend on a vector of p different parameters, $\theta(t) \in \mathbb{R}^p$, where each parameter $\theta_i(t)$ can be decomposed as

$$\forall i \in \{1,\dots,p\},\ \theta_i(t) = \theta_i^0 + \delta_i(t)\theta_i^1,\ \delta_i(t) \in [-1,+1]. \tag{6}$$

Here, θ_i^0 denotes the nominal value of the i-th parameter (in general but not necessarily, its expected mean value), and $\theta_i^1 > 0$ its symmetric amplitude variation. Throughout this paper, the values θ_i^0 and θ_i^1 are assumed to be constant and are grouped in the vectors θ^0 and θ^1, respectively. All plant matrices indexed with Δ depend on θ^0 and θ^1, whereas the remaining matrices depend only on θ^0. Moreover, $\Delta(t)$ is block-diagonal and elementwise bounded, belonging to

$$\mathscr{P}_\Delta = \{\mathrm{blockdiag}(\delta_1\mathbf{I}_{r_1},...,\delta_p\mathbf{I}_{r_p}):\ \delta_i(t) \in [-1,+1]\}, \tag{7}$$

with $1 \leq i \leq p$, $r_i \in \mathbb{N}$ the number of repetitions of the i-th parameter, and $\sum_{i=1}^p r_i = n_\Delta$.

For all time t, $\theta(t)$ belongs to a polytope centred in θ^0, whose edge length in the i-th direction is $2\theta_i^1$. This polytope can be expressed as

$$\mathscr{P}_\theta = \prod_{i=1}^{p}[\theta_i^0 - \theta_i^1; \theta_i^0 + \theta_i^1]. \tag{8}$$

An illustration of this polytope is provided in Fig. 1 for $p = 3$.

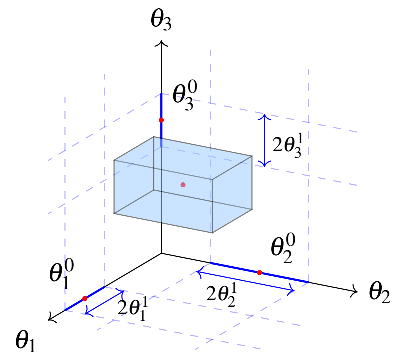

Fig. 1. Uncertainty volume for $p = 3$

It should be noted that the framework presented here is continuous but can be discretized if required, using a First-Order Hold for the uncertain signals $\mathbf{w}_\Delta$ and $\mathbf{z}_\Delta$, and a Zero-Order Hold for the others [10]. All subsequent frameworks and methods remain valid under these assumptions.

2) Polytopic LPV framework: In this case, the uncertainty does not need to be isolated as in the more general LFT formulation. Instead, the state-space matrices depend affinely on the varying parameters :

$$\dot{\mathbf{x}}(t) = \mathbf{A}(\theta(t))\mathbf{x}(t) + \mathbf{B}_1(\theta(t))\mathbf{w}(t) + \mathbf{B}_2\mathbf{u}(t), \tag{9a}$$

$$\mathbf{z}(t) = \mathbf{C}_1(\theta(t))\mathbf{x}(t) + \mathbf{D}_{11}(\theta(t))\mathbf{w}(t) + \mathbf{D}_{12}\mathbf{u}(t), \tag{9b}$$

$$\mathbf{y}(t) = \mathbf{C}_2(\theta(t))\mathbf{x}(t) + \mathbf{D}_{21}(\theta(t))\mathbf{w}(t) + \mathbf{D}_{22}\mathbf{u}(t), \tag{9c}$$

with, for instance,

$$\mathbf{A}(\theta(t)) := \mathbf{A}_0 + \sum_{i=1}^{p}\theta_i(t)\mathbf{A}_i, \tag{10}$$

and $\theta_i(t)$ described in (6). Similar affine dependencies hold for $\mathbf{B}_1(\theta(t))$, $\mathbf{C}_1(\theta(t))$, $\mathbf{C}_2(\theta(t))$, $\mathbf{D}_{11}(\theta(t))$, and $\mathbf{D}_{21}(\theta(t))$. The signals have the same respective dimensions as in (5). This state-space defines a plant denoted G_θ, which is represented in Fig. 2. Here again, Fig. 1 provides a representation of the uncertain volume in which $\theta(t)$ lives for $p = 3$.

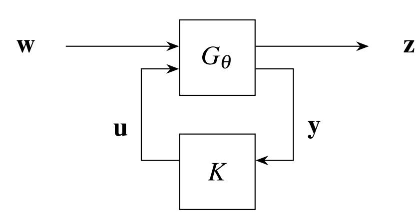

Fig. 2. Robust GS control configuration for the polytopic problem

C. LPV controller synthesis

1) LPV-LFT Controller synthesis: The controller dynamics is obtained with the same parametric dependence on Δ, which leads to the following state-space model

$$\begin{bmatrix} \dot{\mathbf{x}}_K(t) \\ \mathbf{z}_K(t) \\ \mathbf{u}(t) \end{bmatrix} = \begin{bmatrix} \mathbf{A}_K & \mathbf{B}_{K\Delta} & \mathbf{B}_{K1} \\ \mathbf{C}_{K\Delta} & \mathbf{D}_{K\Delta\Delta} & \mathbf{D}_{K\Delta 1} \\ \mathbf{C}_{K1} & \mathbf{D}_{K1\Delta} & \mathbf{D}_{K11} \end{bmatrix} \begin{bmatrix} \mathbf{x}_K(t) \\ \mathbf{w}_K(t) \\ \mathbf{y}(t) \end{bmatrix}, \tag{11a}$$

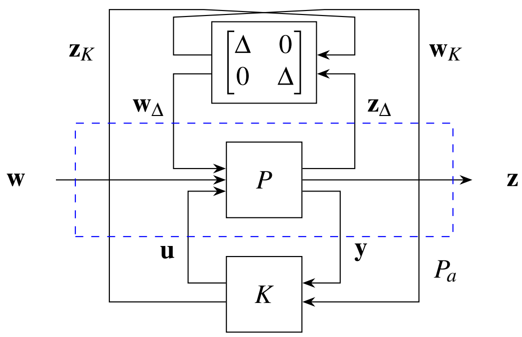

Fig. 3. Robust GS control configuration for the LFT problem

$$\mathbf{w}_K(t) = \Delta(t)\mathbf{z}_K(t), \tag{11b}$$

with $\mathbf{x}_K \in \mathbb{R}^{n_K}$, $\mathbf{w}_K, \mathbf{z}_K \in \mathbb{R}^{n_\Delta}$, $\mathbf{u} \in \mathbb{R}^{n_u}$, and $\mathbf{y} \in \mathbb{R}^{n_y}$. The interconnection diagram is then shown in Fig. 3.

For a certain prescribed performance level $\gamma > 0$, and for all $\Delta(t) \in \mathscr{P}_\Delta$ such that $\|\Delta\|_{\mathscr{L}_2} \leq 1/\gamma$, the LPV-LFT controller synthesis problem consists in determining the controller matrices so that K satisfies

$$\|F_\ell(F_u(P,\Delta), F_\ell(K,\Delta))\|_{\mathscr{L}_2} < \gamma \tag{12}$$

where F_ℓ and F_u denote the lower and upper LFT transformations, respectively.

The problem is solved with the scaled small-gain theorem [3, 4], as recalled in Theorem 1.

Theorem 1 (Scaled Small-Gain): If there exists a scaling symmetric matrix

$$\mathbf{L} = \begin{bmatrix}\mathbf{L}_1 & \mathbf{L}_2\\ \mathbf{L}_2^\top & \mathbf{L}_3\end{bmatrix} \succ \mathbf{0}, \quad \mathbf{L}_i \in \mathbb{R}^{n_\Delta \times n_\Delta}, \tag{13}$$

such that $\forall \Delta(t) \in \mathscr{P}_\Delta, \forall i \in \{1,2,3\}, \mathbf{L}_i\Delta(t) = \Delta(t)\mathbf{L}_i$, with $\mathbf{L}_1 \succ \mathbf{0}, \mathbf{L}_3 \succ \mathbf{0}$; and an LTI control structure K such that the closed-loop system $F_\ell(P,K)$, defined with (5) and (11), is internally stable and which satisfies

$$\left\| \begin{bmatrix}\mathbf{L}^{1/2} & \mathbf{0}\\ \mathbf{0} & \mathbf{I}_{n_z}\end{bmatrix} F_\ell(P_a,K) \begin{bmatrix}\mathbf{L}^{-1/2} & \mathbf{0}\\ \mathbf{0} & \mathbf{I}_{n_w}\end{bmatrix} \right\|_\infty < \gamma, \tag{14}$$

with P_a described in Fig. 3, then $F_\ell(K,\Delta)$ is a γ-suboptimal GS $\mathscr{H}_\infty$-controller.

2) Polytopic LPV Controller synthesis: In the polytopic framework, the GS controller state-space is obtained by solving the three LMIs of Theorem 4.3 of [11] at each vertex of the polytope $\mathscr{P}_\theta$, depending on a certain level of performance γ. Consequently, a controller must be computed for every vertex, which requires solving 3×2^p LMIs whenever the polytope definition changes. The overall GS controller is then reconstructed by interpolation using the polytopic coordinates.

Definition 4 (Polytopic coordinates): Considering a p-dimensional polytope $\mathscr{P}$ defined by $\mathscr{P} = \prod_{i=1}^{p}[\underline{\theta}_i, \overline{\theta}_i]$ and the set of its 2^p vertices $\{\mathbf{s}_1, \ldots, \mathbf{s}_{2^p}\} \subset (\mathbb{R}^p)^{2^p}$, a time-varying vector $\theta(t) \in \mathscr{P}$ can be expressed thanks to its *polytopic coordinates* as follows:

$$\theta(t) = \sum_{i=1}^{2^p} \alpha_i(t)\mathbf{s}_i, \tag{15}$$

where

$$\alpha_i(t) = \frac{\prod_{j=1}^{p} |\theta_j(t) - C(\mathbf{s}_i)_j|}{\prod_{j=1}^{p} |\overline{\theta}_j - \underline{\theta}_j|}, \tag{16}$$

with

$$C(\mathbf{s}_i)_j = \begin{cases}\overline{\theta}_j \text{ if } (\mathbf{s}_i)_j = \underline{\theta}_j\\ \underline{\theta}_j \text{ if } (\mathbf{s}_i)_j = \overline{\theta}_j\end{cases}.$$

Moreover, one can see that for all t and i, $\alpha_i(t) \geq 0$; and $\sum_{i=1}^{2^p} \alpha_i(t) = 1$.

In our case, the polytope $\mathscr{P}_\theta$ is symmetric. We denote by $\mathbf{s}_1, \ldots, \mathbf{s}_{2^p}$ the 2^p $\mathbb{R}^p$-vectors of coordinates of the vertices of $\mathscr{P}_\theta$, *i.e.*, the vectors of the form $\theta_1^0 \pm \theta_1^1, \cdots, \theta_p^0 \pm \theta_p^1$; the polytopic coordinates are simplified and (16) becomes:

$$\alpha_i(t) = \frac{\prod_{i=1}^{p} |\theta_j(t) - C(\mathbf{s}_i)_j|}{2^p \prod_{i=1}^{p} \theta_i^1}, \tag{17}$$

with

$$C(\mathbf{s}_i)_j = \begin{cases}\theta_j^0 + \theta_j^1 \text{ if } (\mathbf{s}_i)_j = \theta_j^0 - \theta_j^1\\ \theta_j^0 - \theta_j^1 \text{ if } (\mathbf{s}_i)_j = \theta_j^0 + \theta_j^1\end{cases}.$$

Then, denoting K_i the controller obtained for the vertex $\mathbf{s}_i$, the GS controller is reconstructed with the same polytopic dependence:

$$K = \sum_{i=1}^{2^p} \alpha_i(t)K_i. \tag{18}$$

The resulting GS controller K is γ-suboptimal, since for a prescribed performance level γ it satisfies

$$\sup_{\theta \in \mathscr{P}_\theta} \|F_\ell(G_\theta, K)\|_{\mathscr{L}_2} < \gamma. \tag{19}$$

In this paper, the α_i are assumed to be measured exactly at all times. Recent studies, however, have addressed the effect of observation errors using model predictive control under slowness assumptions [12].

D. Summary of the contribution

The main contribution of this paper is to maximize both performance and the admissible uncertainty volume simultaneously. In other words, the objective is to minimize γ (satisfying (14) in the LFT framework, (19) in the polytopic one) while maximizing the volume of the polytope in which the uncertain parameters may vary (8) without destabilizing the system. The volume is defined as:

$$V(\theta^1) = 2^p \prod_{i=1}^{p} \theta_i^1. \tag{20}$$

III. Methodology

A. Optimization problem

1) Definitions: The uncertainty volume $V(\theta^1)$ must be normalized to avoid dependence on the physical meaning of the parameters. The scaled volume to maximize, ranging from 0 to 1, is therefore defined as :

$$\widetilde{V}(\theta) = \frac{V(\theta^1)}{2^p \prod_{i=1}^{p} \theta_i^0} = \prod_{i=1}^{p} \frac{\theta_i^1}{\theta_i^0}, \quad \text{with } 0 \leq \theta_i^1 \leq \theta_i^0. \tag{21}$$

The case $\widetilde{V}(\theta) = 1$ corresponds to $\pm 100\%$ variation of each parameter. It should be noted that in practice, physical constraints may prevent $\widetilde{V}(\theta)$ from reaching 1, as in the case $0 \leq \theta_i^1 \leq M_i < \theta_i^0$ in the examples.

The boundaries of parameter variations (collected into the vector θ^1) are the optimization variables. As it is clear that decreasing $V(\theta^1)$ will lead to a smaller γ, and increasing it will necessarily increase γ, a good compromise is obtained with the search for a maximum of $V(\theta^1)/\gamma^p$. That is equivalent to considering the lengths of the polytope edges being $2\theta_i^1/\gamma$, as done with the structured singular value in [7]. Physically, this formulation makes sense as from (6), for any $1 \leq i \leq p$ and t we have:

$$|\theta_i(t) - \theta_i^0| \leq |\delta_i(t)|\theta_i^1. \tag{22}$$

Combining (22) with the small-gain theorem – which necessitates $|\delta_i(t)| \leq 1/\gamma$ to ensure closed-loop stability – finally leads to the stability condition

$$|\theta_i(t) - \theta_i^0| \leq \frac{\theta_i^1}{\gamma}. \tag{23}$$

Moreover, the polytope can be transformed by weighting the scaled volume in (21) with coefficients w_i, thereby prioritizing some uncertain parameter bounds over others in the optimization process.

2) Cost function of the LFT problem: To overcome the numerical sensitivity of LMI techniques, the scaling matrix $\mathbf{L}$ defined in (13) is also an optimization variable, following the idea introduced in [6]. Let us introduce

$$\Lambda(\mathbf{L}) = -\min\left(\lambda_{\min}(\mathbf{L}_1), \lambda_{\min}(\mathbf{L}_3), \lambda_{\min}(\mathbf{L})\right), \tag{24}$$

with $\lambda_{\min}(\cdot)$ the smallest eigenvalue of a matrix. This term is included in the cost function to ensure feasibility of the solutions.

The above considerations, combined with the requirement that $\Lambda(\mathbf{L}) < 0$, lead to the following optimization problem :

$$\min_{\mathbf{L},\theta} f_{\text{LFT}}(\mathbf{L}, \theta) \tag{25a}$$

with cost function

$$f_{\text{LFT}}(\mathbf{L}, \theta) = \begin{cases} \Lambda(\mathbf{L}) & \text{if } \Lambda(\mathbf{L}) \geq 0, \\ -\dfrac{1}{\frac{\gamma(\mathbf{L},\theta)^p}{\widetilde{V}(\theta)} + \beta e^{-(\gamma(\mathbf{L},\theta)-\gamma_{\text{nom}})}} & \text{else.} \end{cases} \tag{25b}$$

Here, β is a user-defined parameter that allows volume maximization or performance to be prioritized (see section III-B for more details). At each iteration, $\gamma(\mathbf{L}, \theta)$, $\Lambda(\mathbf{L})$ and $\widetilde{V}(\theta)$ (satisfying Eqs. (14), (24) and (21)) are computed to evaluate the cost function. γ_{nom} is the $\mathscr{H}_\infty$-norm of the nominal plant P (whose expression is given by (5) but with no perturbation, *i.e.*, $\Delta(t) \equiv \mathbf{0}$). In other terms:

$$\gamma_{\text{nom}} := \|F_\ell(F_u(P, \mathbf{0}), F_\ell(K_\infty, \mathbf{0}))\|_\infty, \tag{26}$$

where K_∞ is a solution of the standard $\mathscr{H}_\infty$-synthesis.

Moreover, the form of the cost function can immediately indicate whether the converged solution is feasible or not: $f_{\text{LFT}}(\mathbf{L}, \theta) < 0$ if and only if $\Lambda(\mathbf{L}) < 0$, which means that the scalings are effectively positive definite as in Theorem 1.

3) Cost function of the polytopic problem: Here the cost function is similar, except that no scaling needs to be computed to ensure stability, so the algorithm can directly focus on performance. In this case,

$$\gamma_{\text{nom}} := \|F_\ell(G_0, K)\|_\infty, \tag{27}$$

where K is obtained from the standard $\mathscr{H}_\infty$-synthesis and G_0 corresponds to the nominal plant G_θ represented in Fig. 2 with constant nominal parameters: $\theta(t) \equiv \theta^0$.

The cost function is then defined as

$$f_{\text{poly}}(\theta) = \frac{\gamma(\theta)^p}{\widetilde{V}(\theta)} + \beta e^{-(\gamma(\theta)-\gamma_{\text{nom}})}, \tag{28}$$

where $\gamma(\theta)$ and $\widetilde{V}(\theta)$ are computed at each iteration according to (19) and (21). As before, β is user-defined.

Here, as no scaling needs to be found, any computed couple $(\gamma(\theta), \tilde{V}(\theta))$ corresponds to a feasible solution, even though this solution may be very conservative (and thus, lead to a very high cost $f_{\text{poly}}(\theta)$).

B. Discussion on the choice of cost functions

The form $\gamma(\theta)^p/\widetilde{V}(\theta) + \beta e^{-(\gamma(\theta)-\gamma_{\text{nom}})}$ that can be found in both cost functions was validated after several empirical tests and is motivated by two main concerns in terms of optimization.

- First, $\gamma(\mathbf{L}, \theta)$ is a single optimization variable while $\tilde{V}(\theta)$ is the product of p optimization variables (see (21) and (23)). Then, it makes sense to compare $\gamma(\mathbf{L}, \theta)^p$, rather than $\gamma(\mathbf{L}, \theta)$, to $\tilde{V}(\theta)$: otherwise the optimization algorithm would mainly focus its search on maximizing the uncertainty volume rather than obtaining a good level of performance.
- Second, as adhering to frequency weighting constraints is paramount in industrial applications, minimizing $\gamma(\mathbf{L}, \theta)$ should be prioritized in the optimization process. This consideration leads to the introduction of the exponential barrier term $\beta e^{-(\gamma(\theta)-\gamma_{\text{nom}})}$, which (the more β is increased) ensures that priority is given to solutions where $\gamma(\mathbf{L}, \theta)$ remains close to the nominal performance γ_{nom}.

Furthermore, both LFT and polytopic cost functions are bounded from below. Indeed, as for physical reasons, $\gamma(\mathbf{L}, \theta) > \gamma_{\text{nom}}$, and $\widetilde{V}(\theta) \leq 1$, the LFT cost function admits the following lower bound :

$$f_{\text{LFT}}(\mathbf{L}, \theta) > -\frac{1}{\gamma_{\text{nom}}^p + \beta}. \tag{29}$$

Similarly, in the polytopic case, the following lower bound holds:

$$f_{\text{poly}}(\theta) > \gamma_{\text{nom}}^p + \beta. \tag{30}$$

C. Metaheuristics

Given the highly non-convex nature of the proposed optimization problem, traditional exact methods are prone to converging toward suboptimal local minima. To overcome this limitation, we turn to a metaheuristic approach. Metaheuristics are high-level, stochastic, and iterative algorithms specifically designed for highly complex problems where exact solutions are computationally prohibitive. By dynamically adapting to the topology of the search space, these strategies range from localized searches to comprehensive global exploration, providing a robust mechanism to approximate the global optimum with minimal problem-specific modifications.

For the present optimization problem, Particle Swarm Optimization [5] is adopted, as it has proven highly effective for robust control design [6]. Other numerical approaches can also be considered, such as genetic algorithms [13], simulated annealing [14], or ant colony optimization [15]. A comprehensive review of metaheuristic methods for robust control is provided in [6].

IV. Benchmark examples and results

Two benchmarks are presented. The LFT framework is more general and does not require LMI resolution, but infinitely many models can represent the same system. It is illustrated with a mechatronic example involving six different varying parameters. The polytopic framework, on the other hand, is more conservative and requires LMI resolution, but the plant representation is unique and simpler. It is illustrated with a cart-pendulum system benchmark with two different varying parameters.

It is worth mentioning that these two separate case studies are each tailored to highlight the specific features of the proposed methods. Given the differences in their mathematical formulations and numerical resolutions, these examples are evaluated independently and are presented for illustrative purposes rather than for comparative analysis.

A. LPV-LFT system benchmark

1) Mechatronic example with a flexible mode : In this first example, a mechatronic model with flexible modes is considered. The system matrices are detailed in Appendix A. Six parameters are time-varying: the electrical resistance R, the viscous friction coefficient F, the spring rate K, the torque coefficient K_c, and the damping ξ and frequency ω_0 of the flexible mode. In the LFT formulation, the torque coefficient must be repeated twice, which yields

$$\Delta(t) = \text{blockdiag}(\delta R, \delta F, \delta K_r, \delta K_c \mathbf{I}_2, \delta\xi, \delta\omega_0). \tag{31}$$

where the explicit dependence on time t of the uncertainties has been omitted for brevity.

In (6) and (7), this corresponds to $p = 6$, $r_1 = r_2 = r_3 = r_5 = r_6 = 1$ and $r_4 = 2$. The nominal parameters grouped in θ^0 are $R^0 = 5.86 \times 10^{-1}\,\Omega$, $F^0 = 2.57 \times 10^{-2}\,\text{N.m.rad}^{-1}$, $K_r^0 = 1.64 \times 10^{-3}\,\text{N.m.rad}^{-1}$, $K_c^0 = 8.46 \times 10^{-4}\,\text{N.m.rad}^{-1}$, $\xi^0 = 2.5 \times 10^{-2}$ and $\omega_0^0 = 3.5\,\text{rad.s}^{-1}$. For confidentiality reasons, these numerical values have been obtained after a change of variables and system normalization; they are therefore not representative of the actual physical parameters.

Consequently, as detailed in [6], in order to verify the assumptions of Theorem 1, the scaling matrices $\mathbf{L}_i$ must be sought in the form

$$\mathbf{L}_i = \text{blockdiag}\left(l_{11}^i, l_{22}^i, l_{33}^i, \begin{bmatrix} l_{44}^i & l_{45}^i \\ l_{45}^i & l_{55}^i \end{bmatrix}, l_{66}^i, l_{77}^i\right), \tag{32}$$

with the l_{kl}^i being the scaling decision variables.

The final controller is computed using the $\mathscr{H}_\infty$-loop-shaping method [16, 17, 18], adapted to the LPV framework. Since the system considered here is SISO, the requirements are satisfied with a single frequency weighting function, provided together with the model in Appendix A.

TABLE I
Summary of the results

Framework System	LFT Mechatronic system	Polytopic Cart-pendulum system
p	6	2
γ_{nom}	2.76	1.07
$\bar{\gamma}$	4.72	1.75
STD(γ)	0.26	0.00
$\bar{\tilde{V}}$	63.65%	19.64%
STD($\tilde{V}$)	20.40%	0.01%
$\bar{t}_{\text{run}}$	7.10 min	1.10 min

2) Results: Twenty runs were performed with a weighting $\beta = 1$ in the cost function defined in (25) and a summary of the results is reported in Tab. I. Mean values and standard deviations of γ and of $\tilde{V}$ are presented, together with the mean computation time.

The uncertain parameters can almost all vary by $\pm 100\%$ while still ensuring the existence of a controller. The limiting parameter is often the motor torque coefficient K_c, which tolerates variations of about $\pm 60\%$ while all other parameters can change freely (see Appendix A for more details on the dynamics model). The mean performance $\bar{\gamma}$ remains relatively close to γ_{nom}, despite the presence of six varying parameters.

The convergence of the algorithm in one of the runs is shown in Fig. 4 (only the 200 first iterations are displayed to better show the important features). Instead of the raw cost function, $\text{symlog}(f_{\text{LFT}}(\mathbf{L}, \theta))$ is displayed to better highlight negative values, with the function symlog defined by $\text{symlog}(y) := \text{sign}(y)\log(1 + |y|/10^{-8})$. Dashed blue lines represent the lower bounds for the cost function ($\text{symlog}(-2.26 \times 10^{-3})$ from (25)) and γ ($\gamma_{\text{nom}} = 2.76$); and the upper bound of $\tilde{V}$, equal to 1. The behaviour of the algorithm described in the methodology section is clearly visible: no feasible solution - i.e., no scaling satisfying (24) - is found during the first 18 iterations. Consequently, the cost remains positive, and computing γ and $\tilde{V}$ is meaningless. From the 19th iteration onward, feasible scalings are found, and the optimization focuses on minimizing γ and maximizing $\tilde{V}$. The barrier term enforces faster convergence of γ, while different values of $\tilde{V}$ are explored over a longer period: the algorithm accepts a smaller uncertainty volume if it allows a better controller to be found within it.

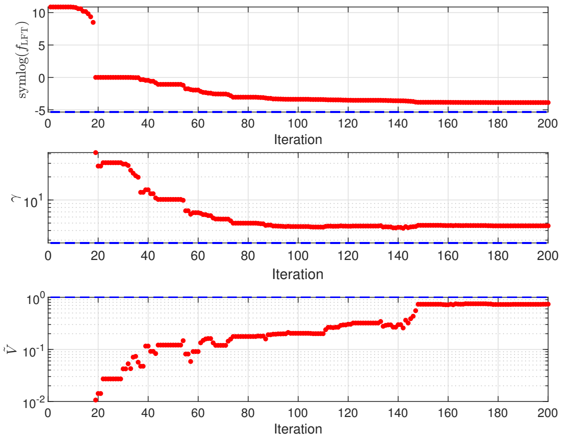

Fig. 4. Convergence of the optimization algorithm on the mechatronic benchmark

B. Polytopic system benchmark

1) Cart-pendulum system: Here, a cart–pole system is considered. Its state-space model is provided in Appendix B. The uncertain parameters are the inverse of the cable length $\tilde{l}$, and the inverse of the motor inertia $\tilde{J}$. Note that these inverses are used because the original physical quantities do not fit the LPV form, whereas their reciprocals can be directly taken as varying parameters. The uncertainty is described by

$$\Delta(t) = \mathrm{blockdiag}(\delta\tilde{l}(t)\mathbf{I}_2, \delta\tilde{J}(t)\mathbf{I}_2), \tag{33}$$

which corresponds to $p = 2$ and $r_1 = r_2 = 2$, according to the notations of (6) and (7). The vector of nominal values θ^0 is given by $\tilde{J}^0 = 2.08 \times 10^5\,\mathrm{kg}^{-1}.\mathrm{m}^{-2}$ and $\tilde{l}^0 = 6.67\,\mathrm{m}^{-1}$.

2) Results: For this example as well, twenty runs were performed with $\beta = 1$ in (28), and the results are again reported in Tab. I. From the matrices in Appendix B, it can be observed that, unlike the previous case, the scaled volume can never reach 100%, since the varying parameters are the inverses of physical quantities (length and inertia): a 100% variation would imply that these parameters could vanish, which is not physically realizable. Consequently, the uncertain volume is limited to about $\pm 20\%$ of the nominal volume. Nevertheless, the mean performance level obtained, $\bar{\gamma} < 3$, indicates a satisfactory closed-loop performance [16, 17, 18]. Furthermore, the standard deviations of both γ and $\tilde{V}$ are close to zero, indicating that all independent runs consistently converged toward a presumed global minimum.

No convergence figure is provided for brevity reasons, but the shape of convergence is similar to Fig. 4 from the iteration when the cost becomes negative, as there is no scaling to be found in the polytopic framework, and the cost function is similar.

C. Computational aspects

The simulations were run on a computer with a Intel Core i9-11900H @2.5GHz processor and 64GB of RAM, under Windows 11. The implementation was performed in Matlab R2024a, using 8 cores for all computations. Mean computation times, denoted $\bar{t}_{\mathrm{run}}$, are reported together with the other results in Tab. I. The Matlab Robust Control Toolbox (`hinfgs` for the polytopic case), Global Optimization Toolbox (`particleswarm`), and Parallel Computing Toolbox were used. For both benchmarks, PSO stopping criteria were set to a maximum of 50 stall iterations and a function tolerance of 10^{-7}. The swarm size was chosen as twice the number of variables.

- Mechatronic example: 30 variables, including 24 scaling variables (since each of the three symmetric matrices $\mathbf{L}_i$ has seven diagonal elements and one off-diagonal element) and six uncertain boundaries $(\theta_i^1)_{1\leq i\leq 6}$;
- Cart–pole example: 2 variables, corresponding only to the uncertainty bounds $(\theta_i^1)_{1\leq i\leq 2}$ (1 for each uncertainty). No scaling variable is required here, since the formulation is polytopic rather than LFT.

V. Conclusion

In this paper, a method for designing an adaptive robust controller for a plant in LPV form is proposed. The main contribution lies in performing gain-scheduled controller synthesis simultaneously with the maximization of the uncertainty polytope volume. The problem is formulated as an optimization task and solved using a metaheuristic algorithm, which searches jointly for a robust controller – through the search for suitable scalings ensuring controller existence via the scaled small-gain theorem, if the system is under LFT form; and through LMI resolution if the system is under polytopic form – and for the largest admissible uncertainty bounds. The approach has been demonstrated on two benchmark systems: a mechatronic example with six uncertain parameters (LFT formulation) and a cart–pole system with two uncertain parameters (polytopic formulation). In both cases, the results show acceptable to good $\mathscr{H}_\infty$ performance while maintaining sufficiently large uncertainty volumes for practical implementation.

Future work will address a multi-objective reformulation of the problem, for instance minimizing γ and $1/\widetilde{V}$ simultaneously to derive a Pareto front.

References

[1] C. Briat. *Linear Parameter-Varying and Time-Delay Systems. Analysis, Observation, Filtering & Control*. Springer-Verlag, 01 2015. ISBN 978-3-662-44049-0.

[2] R. Pédenon-Orlanducci, P. Feyel, and D. Saussié. LPV-LFT Synthesis Approach for Non-Conservative Stability Conditions with Integrated Identifier (Extended Abstract). In *9th IFAC Systems Structures and Control Conf.*, 2025.

[3] A. Packard. Gain scheduling via linear fractional transformations. *Systems & Control Letters*, 22(2):79–92, 1994. ISSN 0167-6911.

[4] P. Apkarian and P. Gahinet. A Convex Characterization of Gain-Scheduled Hinf Controllers. *IEEE Transactions on Automatic Control*, 40:853 – 864, 06 1995.

[5] J. Kennedy and R. Eberhart. Particle swarm optimization. In *Proceedings of ICNN'95 - International Conf. on Neural Networks*, volume 4, pages 1942–1948, 1995.

[6] P. Feyel. *Robust Control Optimization with Metaheuristics*. Wiley, ISTE edition, 2017. ISBN 978-1-78630-042-3.

[7] G. Sandou. Maximization of the volume of the mu guaranteed stability domain using Particle Swarm Optimization. In *2014 European Control Conf. (ECC)*, pages 582–587, 2014.

[8] M.Kada, A. Kameche, A. Heddar, and A. Mennouni. Some new results about the stability radius of infinite-dimensional systems perturbed stochastically and deterministically. *International Journal of Control*, 98(4):944–957, 2025.

[9] K. Zhou, J. Doyle, and Glover K. *Robust and Optimal Control*. Prentice Hall, 1996. ISBN 978-0-134-56567-5.

[10] R. Tóth, M. Lovera, P. S. C. Heuberger, and P. M. J. Van den Hof. Discretization of linear fractional representations of LPV systems. In *Proceedings of the 48h IEEE Conf. on Decision and Control (CDC) held jointly with 28th Chinese Control Conf.*, pages 7424–7429, 2009.

[11] G. Becker and A. Packard. Robust performance of linear parametrically varying systems using parametrically-dependent linear feedback. *Systems & Control Letters*, 23(3):205–215, 1994. ISSN 0167-6911.

[12] H. Esfahani and S. Gros. Policy gradient reinforcement learning for uncertain polytopic lpv systems based on MHE-MPC. *IFAC-PapersOnLine*, 55(15):1–6, 2022. ISSN 2405-8963. 6th IFAC Conf. on Intelligent Control and Automation Sciences ICONS 2022.

[13] D. Goldberg. *Genetic Algorithm in Search, Optimization and Machine Learning*. Addison-Wesley, 1989. ISBN 0-201-15767-5.

[14] S. Kirkpatrick, C. D. Gelatt, and M. P. Vecchi. Optimization by simulated annealing. *Science*, 220(4598):671–680, 1983.

[15] M. Dorigo, V. Maniezzo, and A. Colorni. Ant system: Optimization by a colony of cooperating agents. *IEEE Transactions on Systems, Man, and Cybernetics, Part B (Cybernetics)*, 26(1):29–41, 1996.

[16] D. McFarlane and K. Glover. *Robust controller design using normalized coprime factor plant descriptions*. Springer, Berlin, Heidelberg, 1990. ISBN 978-3-540-46828-8.

[17] D. McFarlane and K. Glover. A loop-shaping design procedure using H/sub infinity / synthesis. *IEEE Trans. Automat. Contr*, 37(6):759–769, 1992.

[18] P. Feyel. *Loop-Shaping Robust Control*. Wiley, ISTE edition, 2013. ISBN 978-1-84821-465-1.

Appendix

A. Mechatronic system with flexible mode (LFT case)

The matrices of the LFT representation can be readily derived from the dynamical equations of the following system, whose state vector is $\mathbf{x} = [i\ \theta_a\ \omega_a\ \theta_1\ \omega_1]^\top$.The output is $x_2 + x_4$ and the input u. The dynamics are assumed to be slow enough to neglect the counter-electromotive force.

$$
\begin{aligned}
\dot{x}_1(t) &= -\frac{R(t)}{L}x_1(t) + \frac{1}{L}u(t),\\
\dot{x}_2(t) &= x_3(t),\\
\dot{x}_3(t) &= \frac{K_c(t)}{J}x_1(t) - \frac{K_r(t)}{J}x_2(t) - \frac{F(t)}{J}x_3(t),\\
\dot{x}_4(t) &= x_5(t),\\
\dot{x}_5(t) &= a\omega_0(t)^2K_c(t)x_1(t) - \omega_0(t)^2x_4(t) - 2\xi(t)\omega_0(t)x_5(t).
\end{aligned}
$$

The last equation must be linearized because it contains products of uncertain terms. The constant (normalized) coefficients are provided in in Tab. II (part A), and the weighting function for the SISO system is defined by the following transfer function:

$$
W(s) = \frac{2596.1(s+0.02)(s+0.1)(s^2+0.56s+0.16)(s^2+0.24s+144)}{s(s+0.06)(s+1.8)^2} \times \frac{(s^2+0.765s+11.56)(s^2+0.36s+324)(s+20)^2}{(s^2+2.52s+3.24)(s^2+1.201s+16.02)(s^2+12.32s+237.2)^2}.
$$

B. Cart-pendulum system (Polytopic case)

The system is illustrated in Fig. 5, and the control synthesis scheme in Fig. 6. The physical state vector is $\mathbf{x} = [i\,\omega\,x_c\,\varphi\,v_l]^\top$. The frequency weightings are defined as

$$W_\varepsilon = (500s+866)/(1000s+0.866);$$

TABLE II

CONSTANT NUMERICAL VALUES OF THE EXAMPLES

	Quantity	Notation	Value
Ex. A	Inductance	L	0.1 H
	Inertia	J	1.23 kg.m^2
	Flexible mode gain	a	0.09 rad.N^{-1}.m^{-1}
Ex. B	Resistance	R	2.3Ω
	Inductance	L	2×10^{-4} H
	Torque coefficient	ϕ	16.2×10^{-3} V.rad^{-1}.s
	Friction coefficient	f	6.5×10^{-5} N.m.s
	Radius of the pulley	r	2.2×10^{-2} m
	Reduction ratio	N	17
	Cable friction coefficient	α	0.3 m.s^{-1}
	Gravity acceleration	g	9.81 m.s^{-2}
	Position sensor gain	k_x	39.77 V.m^{-1}
	Angle sensor gain	k_φ	4.77 V.m^{-1}

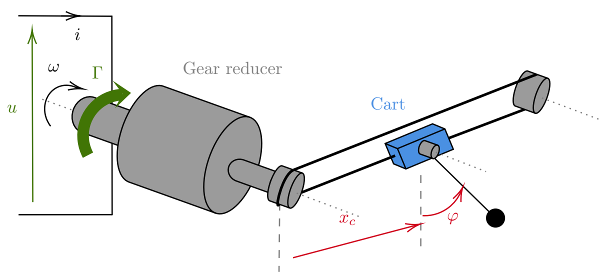

Fig. 5. Cart-pendulum system

$$W_u(s) = (99.5s+200)/(0.995s+2000);$$

$W_\Gamma = 0.01$; $W_\varphi = 2$; $W_{bx} = 1$ and $W_{b\varphi} = 0.1$. The state matrices in (9) can then be reconstructed by augmenting the following ones, where only $\mathbf{A}$ depends on the uncertain parameters $\tilde{J}$ and $\tilde{l}$:

$$
\mathbf{A} = \begin{bmatrix} -\frac{R}{L} & -\frac{\phi}{L} & 0 & 0 & 0\\ \phi\tilde{J} & -f\tilde{J} & 0 & 0 & 0\\ 0 & r/N & 0 & 0 & 0\\ 0 & 0 & 0 & 0 & \tilde{l}\\ -\frac{r\phi\tilde{J}}{N} & \frac{rf\tilde{J}}{N} & 0 & -g & -\alpha\tilde{l} \end{bmatrix}; \mathbf{B}_\Gamma = \begin{bmatrix} 0\\ -1\\ 0\\ 0\\ r/N \end{bmatrix}; \mathbf{B}_u = \begin{bmatrix} 1/L\\ 0\\ 0\\ 0\\ 0 \end{bmatrix}.
$$

The physical input vector is $[\Gamma, u]^\top$, and the outputs are $v_x(t) = k_x x_c(t)$ and $v_\varphi(t) = k_\varphi \varphi(t)$. Detailed developments of this model can be found in Chapter 2 of [6] or in [7] for a slightly simpler version. The numerical values of the constant coefficients are provided in Tab. II (part B).

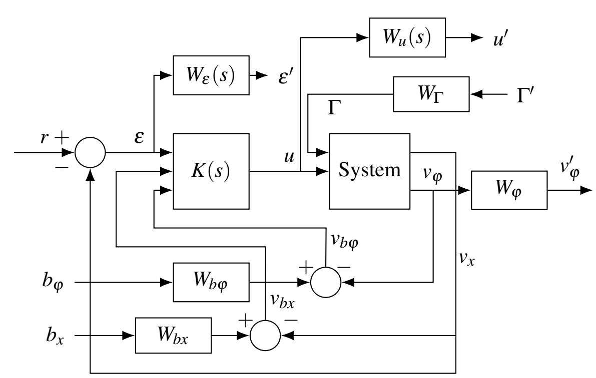

Fig. 6. Control synthesis scheme of the cart-pendulum system